Causality analysis defines neural streams of orienting and holding of attention

Takashi J. Ozaki[a] and Seiji Ogawa[b,c]

Previous studies with effective connectivity analysis have revealed neural streams of orienting of attention. However, neural streams involved in holding of attention on the fovea remain unclear. To identify them, we performed event-related functional MRI with a cueing paradigm and Granger causality analysis. Typical regions along the dorsal attention network (DAN) showed greater activation during orienting than during holding of attention. However, causality analysis indicated that neural streams appeared along the DAN in a top–down manner during orienting, whereas streams from widely distributed regions to the left prefrontal cortex appeared and these were dissociable from the DAN during holding of attention. Our results suggest that dissociable neural streams contribute to orienting and holding of attention, respectively.
NeuroReport **20:1371–1375**

NeuroReport 2009, **20:**1371–1375

Keywords: dorsal attention network, effective connectivity, functional magnetic resonance imaging, Granger causality, holding, orienting, visual attention

[a]Laboratory for Dynamics of Emergent Intelligence, RIKEN Brain Science Institute, Wako, Saitama, [b]Kansei Fukushi Research Center, Tohoku Fukushi University, Sendai, Miyagi and [c]Ogawa Laboratories for Brain Function Research, Hamano Life Science Research Foundation, Shinjuku, Tokyo, Japan

Correspondence to Takashi J. Ozaki, Laboratory for Dynamics of Emergent Intelligence, RIKEN Brain Science Institute, 2-1 Hirosawa, Wako, Saitama 351-0198, Japan
Tel: +81 48 462 1111 x7427; fax: +81 48 467 6938;
e-mail: ozt@brain.riken.jp

Received 17 July 2009 **accepted** 23 July 2009

Introduction

It has been suggested that orienting of attention is mediated by the dorsal attention network (DAN) composed of the human frontal eye field (hFEF) and the dorsal posterior parietal cortex (PPC) [1,2], and that reorienting is mediated by the ventral attention network composed of the inferior frontal cortex and the ventral PPC [3,4]. Studies based on effective connectivity, for example, Granger causality (GC) [5,6], have also suggested that neural streams along the DAN may contribute to the control of orienting of attention in a top–down manner [7].

Many previous studies investigated the difference between neural correlates of orienting/reorienting of attention and those of holding of attention based on neural activations only, and this may be the case for many studies to come. Despite the fact that recent advances in effective connectivity analysis have enabled investigators to clarify the details of neural streams [5,6] and the fact that other studies suggested that visual attention can be controlled by neural streams rather than single functional regions [8,9], the difference of neural streams of orienting of attention and those of holding of attention on the fovea has still received little attention.

Here, we performed event-related functional MRI (fMRI) with the typical Posner's paradigm and GC analysis to identify and determine the differences between the neural streams appearing during orienting and during holding of attention.

Methods

Participants

Six healthy and neurologically normal volunteers (male, right-handed, 23–26 years old) with normal or corrected-normal vision participated in this study. All participants gave their written informed consent, and the study protocol was approved by the Institutional Review Board of Ogawa Laboratories for Brain Function Research in accordance with the Declaration of Helsinki.

Stimuli and procedure

A gray cue template and two Gabor patches colored low-contrast green and red were projected onto a screen, which the participants viewed through a mirror mounted on the head coil of the MRI scanner. The Gabor patches (diameter: 4°) were projected continuously at the right and left positions in two upper quadrants in the visual field (Fig. 1a). The center of each Gabor patch was 4° from the fixation cross, and the size of the cue template was $2 \times 2^{\circ}$ (Fig. 1b).

To begin a trial, a fixation cross appeared in the central visual field, which was followed 4000 ms later by a 'spatial cue' comprising of a horizontal black line with a descending vertical black line either at its left or right end indicating the left or right Gabor patch, respectively, or

0959-4965 © 2009 Wolters Kluwer Health | Lippincott Williams & Wilkins DOI: 10.1097/WNR.0b013e3283313ef3

Fig. 1

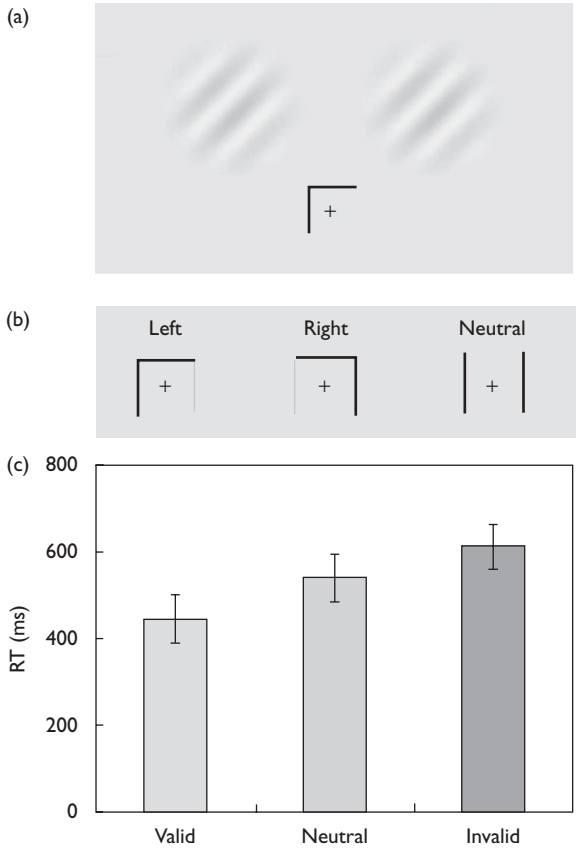

(a) Schematic representation of a cue stimulus indicating leftward. Participants were asked to pay attention to the left Gabor patch. (b) Three types of cues (left, right, and neutral). (c) Mean response time (RT) in each attentional condition. Error bars show SEM.

a 'neutral cue' comprising of both the left and right descending vertical black lines without the horizontal line. The participants were instructed to attend the cued location, that is, the particular Gabor patch (spatial cue) or the fixation cross (neutral cue), while withholding manual responses and saccades (Fig. 1a and b). The cue disappeared 100 ms after the onset and participants were asked to hold their attention on the cued location. After a period of 6000 or 8000 ms assigned randomly to avoid anticipation, the color of one of the Gabor patches was reversed (red to green/green to red) and the participants had to press a button with their right index finger as soon as possible in response.

Trials were classified into four conditions: valid, invalid, neutral, and empty. In the valid condition, the Gabor patch indicated by the spatial cue reversed color (33.3% of trials). In the invalid condition, the Gabor patch that was not indicated by the spatial cue reversed color (8.3%). The cue validity was approximately 75%. In the neutral condition, participants were instructed to hold their attention on the fixation cross until one of the Gabor patches reversed color (16.7%). In the empty condition, no cue appeared prior to one of the Gabor patches reversing color regardless of its location (16.7%). In the catch trials, neither of the Gabor patches reversed color following disappearance of the cue and the participants had to withhold their response (25.0%). Participants performed all trials in a random sequence. The two spatial cues and the neutral cue were presented randomly and with the same probability of occurrence. Based on the cost–benefit paradigm, the cost was defined as the response time (RT) in the invalid condition minus that in the neutral condition, and the benefit as neutral RT minus valid RT.

Functional MRI data acquisition

fMRI data were acquired with a Magnetom Allegra 3.0 T MRI scanner system (Siemens, Erlangen, Germany). The functional volume was acquired with a single-shot echo-planar imaging sequence (repetition time = 1000 ms, echo time = 30 ms, field of view = 224 × 224 mm, voxel size = 3.5 × 3.5 × 7.0 mm, 16 contiguous transverse slices, flip angle = 70°) for each participant. Each scan consisted of 72 runs, each of which consisted of 20 volumes. The anatomical volume was acquired using a magnetization prepared rapid acquisition gradient echo sequence for each participant (voxel size = 1.0 × 1.0 × 1.0 mm). Each anatomical volume was transformed into a standard stereotaxic atlas space based on Talairach coordinates [10].

Functional MRI data analysis

fMRI data were analyzed and visualized using BrainVoyagerQX (Brain Innovation, Maastricht, The Netherlands). The first four volumes of each functional scan were discarded to allow stabilization of magnetization. After correction for slice scan time and head motion within a volume, functional volumes were coregistered with the Talairach space anatomical data sets to generate volume time courses. Each functional scan was high-pass filtered at three cycles per scan. Each voxel was spatially smoothed with a Gaussian filter of 7.0 mm full width at half maximum.

General linear models were fitted to compute statistical parametric maps of the effects of the experimental conditions. The regressors were designed by convolving a square wave function representing the event time course of the cues and targets with a canonical hemodynamic response function. To detect orienting-related neural activation [linear contrast as (valid > neutral)], fixed effects analysis was performed in which the P value threshold was set at P value less than 0.05 (Bonferroni's correction, based on the volume of gray matter).

Regions of interest (ROIs) were determined from the obtained activation map based on the following criteria: (i) activated at a significance level of P value less than 0.0005 (corrected), (ii) volume size greater than 50 mm^3.

A representative anatomical volume was transformed into inflated and rendered three-dimensional images by BrainVoyagerQX (Brain Innovation), on which computed group activation maps were overlaid.

Granger causality analysis

To compute and evaluate causal flows between ROIs, we computed GC using Seth's causal connectivity toolbox based on multivariate autoregressive (VAR) models including lags of multiple time-series [5]. Such a causality analysis based on VAR models can obtain an independent causal index between time-series X_1 and X_2 even if other variables $X_3 \ldots X_N$ can be possible mediators of the causal flow between X_1 and X_2, because VAR model takes all other variables ($X_3 \ldots X_N$) into account and computes the causal index between X_1 and X_2 considering effects of all other variables (see Ref. [5]). Consequently, obtained causality indices exclude any effects of possible mediators ($X_3 \ldots X_N$).

GC analysis was performed in two steps: individual level and subsequent group level. In both the levels, bootstrap methods were applied to evaluate empirical statistical significance [6]. Before the analysis, the time course of averaged blood oxygen level-dependent (BOLD) signals across all voxels in each ROI was extracted.

On an individual level, sample F-values were first computed in both the directions between the measured BOLD time series collapsed across trials of every ROI pair, for each participant in both the cases of orienting and holding, respectively. Each F-value indicates the probability that a BOLD time series of one ROI can explain the subsequent time series of the other ROI [6]. Second, to obtain an empirical null distribution, a bootstrap method was performed for each individual, in which 1000 trial-randomized BOLD time series of each ROI were computed [7]. Third, individual Z-values (Zi) were computed by the rank–Þsum test comparing the sample F-value with the empirical null distribution of F-values for each ROI pair and direction. The Zi obtained for each pair of ROIs and direction from each participant indicated the probability of causality.

At the group level, a combined group Z-value (Zg) was first computed using the Stouffer method for each pair of ROIs and direction (adding all Zi for each pair of ROIs and direction and dividing the sum by the square root of the number of participants) [11]. Second, to estimate the empirical threshold for Zg, a group-level bootstrap method was performed in which 10 000 bootstrap samples of Zg collapsed across ROIs and participants were computed as the empirical null distribution of Zg, and the empirical threshold ($P < 0.05$) was then determined as Zt. Finally, a causality index for each pair of ROIs and direction was assigned a value of 1 ($Zg > Zt$) or 0 ($Zg \leq Zt$). Thus, the index could have a value of 0 (no causality), 1 (unidirectional causality), or 2 (bidirectional causality, i.e., reciprocal interaction).

Causality indices were plotted as network graphs in which directional causalities and reciprocal interactions were described by green unidirectional arrows and by red bidirectional arrows, respectively.

Results

Behavior

Electrooculography recorded in a training session before the fMRI session confirmed stable fixation of each participant. Figure 1c shows mean RT of the participants in the imaging sessions under the valid/neutral/invalid conditions (see Methods). The details were as follows (mean ± SEM): 444 ± 54 ms (valid), 541 ± 55 ms (neutral), and 613 ± 51 ms (invalid). Statistical analyses indicated significant cost–benefit effects of attention (cost: $t_5 = 2.73$, benefit: $t_5 = 3.54$; both $P < 0.05$, Student's t test).

Functional MRI

General linear models analysis showed that typical regions along the DAN and other regions were significantly activated during orienting than during holding of attention ($P < 0.05$, Bonferroni's correction; Fig. 2, gray and black regions), consistent with previous findings [2].

Granger causality analysis

Among all activated clusters, 15 regions were selected as ROIs (Fig. 2, black regions only) and causality indices describing GCs between the ROIs were computed (see Methods). The details of all ROIs are shown in Table 1.

Fig. 2

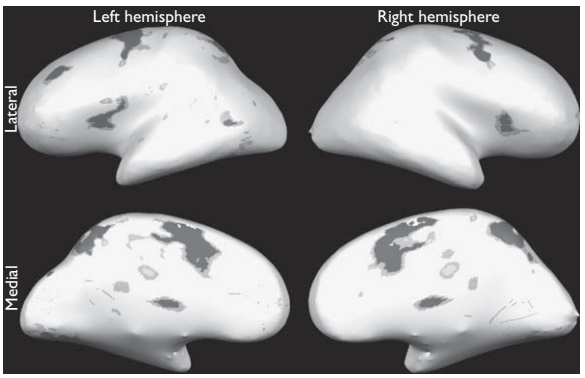

Group maps showing activations during orienting greater than during holding of attention (black and gray regions). The statistical threshold was $P < 0.05$ (Bonferroni's correction). The regions shown in black were selected as regions of interest ($P < 0.0005$, corrected). See Table 1 for details.

Figures 3a and b show network graphs of inter-regional influences among the DAN during orienting and during holding of attention, respectively. These graphs clearly indicate a difference between orienting and holding of attention; there were causal flows from the bilateral hFEF to the ipsilateral visual cortices and either the contralateral or ipsilateral PPC during orienting of attention, consistent with the previous observations of Bressler *et al.* [7], whereas during holding of attention, the left middle frontal gyrus (LMFG) predominantly received causal flows from the contralateral visual cortex and medial frontal cortex, and from the ipsilateral visual cortex and thalamus. During holding of attention, a reciprocal interaction appeared between the LMFG and the left V4. There was no overlap of causal flows between orienting and holding of attention. Importantly, the top–down influences from the hFEF to the PPC and other lower regions did not appear during holding of attention.

Table 1 Details of all ROIs of activation for GC analysis

	Talairach coordinates				
ROI name	*x*	*y*	*z*	Volume (mm^3)	*t*-value
R hFEF	31	−5	53	2631	8.68
R PPC	9	−57	53	4600	9.42
R mFC	7	4	46	3865	9.15
R IFG-AIC	34	18	12	697	7.00
R V4	18	−66	−11	692	7.23
R thalamus	1	−12	9	330	7.57
L hFEF	−27	−8	55	3850	10.41
L PPC	−12	−60	52	5885	9.63
L mFC	−2	−3	46	3230	9.17
L MFG	−30	36	39	911	8.19
L FO-AIC	−35	5	14	1348	7.95
L thalamus	−1	−12	9	250	7.15
L V2	−20	−68	−11	2123	8.04
L V4	−36	−55	−15	1270	7.56
L LOC	−53	−58	14	331	7.39

GC, Granger causality; FO-AIC, frontal operculum-anterior insular cortex; hFEF, human frontal eye field; IFG-AIC, inferior frontal gyrus-anterior insular cortex; L, left; LOC, lateral occipital cortex; mFC, medial frontal cortex; MFG, middle frontal gyrus; PPC, posterior parietal cortex; R, right; ROI, region of interest.

Figures 3c and d show the GC graphs for each condition overlaid on a transparent and three-dimensional rendered gray matter volume and the ROIs for visualization.

Discussion

Our fMRI data and the results of causality analysis indicated that dissociable causal flows define different neural streams for orienting and holding of attention, respectively. To our knowledge, this is the first study of a neural stream for holding of attention composed of

Fig. 3

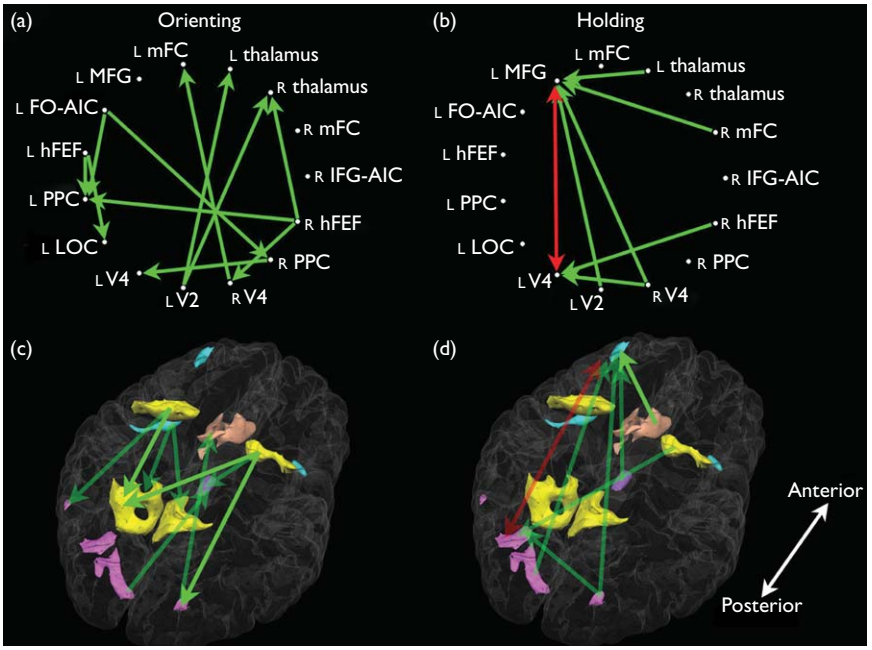

Network graphs obtained from Granger causality (GC) analysis. (top row) The network graph of GC during orienting of attention (a) and that during holding of attention (b). Green unidirectional arrows indicate directional causal flows and red bidirectional arrows indicate reciprocal interactions. (bottom row) The network graph of GC during orienting of attention (c) and holding of attention (d) overlaid on a transparent and three-dimensional-rendered gray matter volume. Faded arrows indicate causal flows passing through the gray matter volume. Regions along the dorsal attention network N are shown in yellow, the visual cortices in pink, the medial frontal cortex in salmon pink, thalami in purple, and other regions including the left middle frontal gyrus (LMFG) are shown in blue. See Table 1 for information about the regions of interest and abbreviations. FO-AIC, frontal operculum–anterior insular cortex; hFEF, human frontal eye field; IFG-AIC, inferior frontal gyrus-anterior insular cortex; L, left; LOC, lateral occipital cortex; mFC, medial frontal cortex; PPC, posterior parietal cortex; R, right; ROI, region of interest.

a stream from the visual cortices, the medial frontal cortex, and the thalamus to the LMFG, which is a part of the lateral prefrontal cortex (LPFC). The neural stream for orienting of attention was also identified as that from the hFEF to the PPC (along the DAN), the visual cortices, and other regions.

The findings of this study regarding the neural stream of orienting of attention were consistent not only with human fMRI evidence [7], but also the results of a nonhuman primate study indicating an interaction between the FEF and V4 during an attentional task [12,13]. The observed connections between the hFEF and the thalami were also consistent with the results of previous neurophysiological studies [14,15]. Evidence of neural streams from the hFEF to the PPC and other regions confirmed that orienting of attention is driven in a top–down manner; the hFEF controls the PPC, V4, and other areas to drive orienting.

In contrast, the LPFC, as the center of the stream for holding of attention, has been suggested to be involved in inhibitory control [16–19]. A previous study indicated that the interaction between the LPFC and the visual cortices enhances foveal attention and inhibits processing of peripheral distractors [20]. From a psychophysical perspective, the process of holding attention entails three functions: engaging attention at the fovea, inhibiting attention from disengaging, and anticipating subsequent stimuli [21]. Therefore, we speculated that the LPFC plays a role in inhibiting attention from disengaging. The reciprocal interaction between the LPFC and the left V4 may be a candidate for a link in such inhibitory control.

In this study, the defined neural streams were restricted within the DAN because ROIs for orienting or holding of attention outside the DAN could not be determined from the present data. Future studies to clarify the entire profiles of the neural streams associated with orienting and holding of attention will require other types of task, such as the attentional network test [22].

Conclusion

Using an event-related fMRI and GC analysis, we identified two different neural streams that appeared during orienting and holding of attention, respectively. The neural streams associated with orienting extended from the bilateral hFEF to the bilateral PPC and other low-level functional structures, including the visual cortices, whereas those associated with holding of attention extended from various functional structures to the left LPFC. Our results indicate that dissociable neural streams are involved in orienting and holding of attention.

Acknowledgements

The authors thank C. Kuroki and M. Kamba for their technical support, and T. Takeda and M. Kawasaki for their valuable comments. This study was supported by Hamano Life Science Research Foundation.

References

1 Corbetta M, Kincade JM, Shulman GL. Neural systems for visual orienting and their relationships to spatial working memory. *J Cogn Neurosci* 2002; **14**:508–523.
2 Corbetta M, Shulman GL. Control of goal-directed and stimulus-driven attention in the brain. *Nat Rev Neurosci* 2002; **3**:201–215.
3 Corbetta M, Patel G, Shulman GL. The reorienting system of the human brain: from environment to theory of mind. *Neuron* 2008; **58**:306–324.
4 Ozaki TJ, Ogawa S, Takeda T. Dissociable neural correlates of reorienting within versus across visual hemifields. *Neuroreport* 2009; **20**:497–501.
5 Seth AK. Causal connectivity of evolved neural networks during behavior. *Network* 2005; **16**:35–54.
6 Roebroeck A, Formisano E, Goebel R. Mapping directed influence over the brain using Granger causality and fMRI. *Neuroimage* 2005; **25**:230–242.
7 Bressler SL, Tang W, Sylvester CM, Shulman GL, Corbetta M. Top-down control of human visual cortex by frontal and parietal cortex in anticipatory visual spatial attention. *J Neurosci* 2008; **28**:10056–10061.
8 Bartolomeo P, Thiebaut de Schotten M, Doricchi F. Left unilateral neglect as a disconnection syndrome. *Cereb Cortex* 2007; **17**:2479–2490.
9 Corbetta M, Kincade MJ, Lewis C, Snyder AZ, Sapir A. Neural basis and recovery of spatial attention deficits in spatial neglect. *Nat Neurosci* 2005; **8**:1603–1610.
10 Talairach J, Tournoux P. *Co-planar stereotaxic atlas of human brain*. Theime New York: Medical Publishers; 1988.
11 Rosenthal R. Writing meta-analytic reviews. *Psychol Bull* 1995; **118**:183–192.
12 Gregoriou GG, Gotts SJ, Zhou H, Desimone R. High-frequency, long-range coupling between prefrontal and visual cortex during attention. *Science* 2009; **324**:1207–1210.
13 Moore T, Armstrong KM. Selective gating of visual signals by microstimulation of frontal cortex. *Nature* 2003; **421**:370–373.
14 Crick F. Function of the thalamic reticular complex: the searchlight hypothesis. *Proc Natl Acad Sci USA* 1984; **81**:4586–4590.
15 McAlonan K, Cavanaugh J, Wurtz RH. Guarding the gateway to cortex with attention in visual thalamus. *Nature* 2008; **456**:391–394.
16 Dias R, Robbins TW, Roberts AC. Dissociation in prefrontal cortex of affective and attentional shifts. *Nature* 1996; **380**:69–72.
17 Kerns JG, Cohen JD, MacDonald AW III, Cho RY, Stenger VA, Carter CS. Anterior cingulate conflict monitoring and adjustments in control. *Science* 2004; **303**:1023–1026.
18 Knight RT, Staines WR, Swick D, Chao LL. Prefrontal cortex regulates inhibition and excitation in distributed neural networks. *Acta Psychol (Amst)* 1999; **101**:159–178.
19 MacDonald AW III, Cohen JD, Stenger VA, Carter CS. Dissociating the role of the dorsolateral prefrontal and anterior cingulate cortex in cognitive control. *Science* 2000; **288**:1835–1838.
20 Tsushima Y, Sasaki Y, Watanabe T. Greater disruption due to failure of inhibitory control on an ambiguous distractor. *Science* 2006; **314**: 1786–1788.
21 Wright RD, Ward LM. *Orienting of attention*. New York: Oxford University Press; 2008.
22 Fan J, McCandliss BD, Sommer T, Raz A, Posner MI. Testing the efficiency and independence of attentional networks. *J Cogn Neurosci* 2002; **14**:340–347.